Sub-basalt imaging in Padra Field, South Cambay Basin, India through sub-surface angle domain processing

Abhinandan Ghosh[1]*, Debkumar Chatterjee[1] and C.P.S. Rana[1]

[1]*SPIC, GPS, WOB, ONGC, Mumbai*

**ghosh_a1@ongc.co.in*

Abstract

Penetration of seismic energy below basalt and generation of sub-basalt imaging has always been a challenging task for seismic exploration. Strong inter-bed multiples always mask the weak reflections coming from sub-basalt formations. Severe scattering of seismic energy due to heterogeneity of basalt layer further complicates the problem which results in the lowering of frequency content of the data and also velocity model building for imaging becomes highly challenging. Padra Field in South Cambay Basin, India is no different, where basaltic Deccan Trap is the technical basement. Conventional PSTM vintages of this area imaged shallow sedimentary part only without much success in imaging the sub-basalt part.

These challenges have been addressed and successful sub-basalt imaging is being achieved through full azimuth sub-surface angle domain processing. In this paper we describe a workflow designed to better image the basement, and fine scale features within the basement, at Padra Field.

Introduction

Sub-basalt imaging continues to provide a challenge in the Padra area. The ability to image seismically the subsurface below the basalts is limited by the fact that basaltic layers are characterized by the poor penetration because of high reflectivity contrasts at the top of the basalt and also due to intra basalt discontinuities, attenuation and strong internal scattering of seismic energy due to heterogeneity of basalt layer resulting lowering of the frequency content of the seismic data. Additionally, the high reflectivity of the basalt-sediment interface generates multiples that contaminates the primary reflections. Building a velocity model which can accurately map the whole volcanic succession as well as the sub-basalt sediment is another challenging task using this kind of weak signal. Enhancing the sub-basalt signal is therefore an element for its imaging.

The Cambay Basin was considered to be formed during Early Cretaceous time due to rifting along Dharwarian orogenic trends during the northward migration of the Indian plate after its break up from Gondwanaland in Late Triassic - Early Jurassic time (Biswas, 1982). Cambay Basin is subdivided into five major tectonic blocks based on major basement faults which have been named from north to south are: (i) Sanchor-Patan Block, (ii) Mehsana-Ahmedabad Block, (iii) Tarapur-Cambay Block, (iv) Jambusar-Broach Block, (v) Narmada-Tapti Block. For the present study area, the Padra structure lies in the north eastern rising flank of the Late Tertiary Broach depression in the South Cambay Basin (Figure 1). The stratigraphic succession of the Padra field is in consonance with South Cambay Basin except that pinching/thinning of the stratigraphic units have been noticed due to Basinal margin position of the field. The drilling results of Padra Field have indicated that Deccan Traps (Cretaceous age) are un-conformably overlain by Olpad Formation (Paleocene), which in turn are also un-conformably overlain by Ankleshwar Formation of Middle to Upper Eocene age followed by other younger sediments. The main hydrocarbon producers of the field are weathered and fractured Deccan Traps and Olpad Formation in addition to Ankleshwar sands. Padra structure shows a series of NNW-SSE trending normal faults almost parallel to one another (Figure 2) forming successive horsts and grabens and thus resulting in series of fault blocks and many fault closures within in the Padra structure. In general, wells lying on the horsts are oil-bearing while those falling in grabens are dry in the basement.

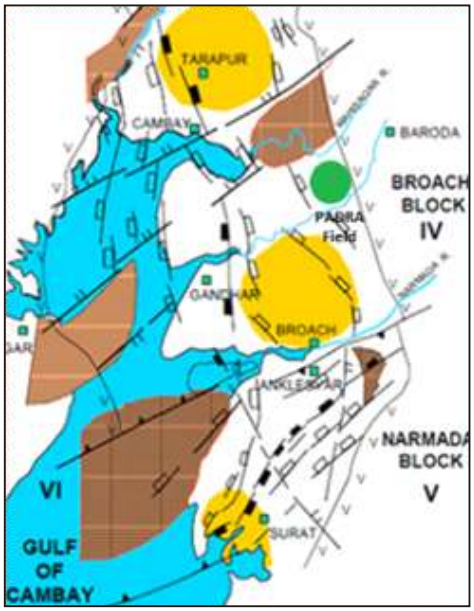

Figure 1: Location map of Padra Field in Broach Block of Cambay Basin.

In full-azimuth sub-surface angle domain processing, an advanced depth imaging system is implemented that first maps the full recorded seismic data into subsurface grid points and then decomposes the data into four-dimensional local

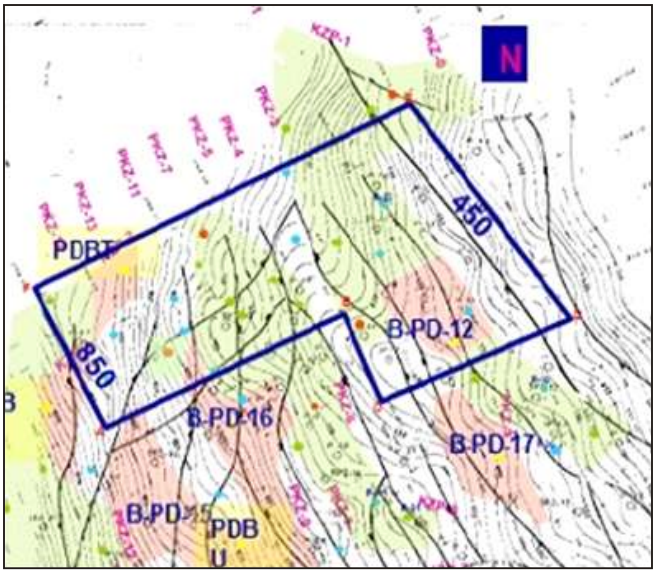

Figure 2: Major fault trends within the study area.

(subsurface) angle domain bins at each point. The mapping and binning are performed using special bottom-up diffraction ray tracing where each seismic event associated with a given image point is related to a given primary ray pair consists of a 'source ray' and a corresponding 'receiver ray'. It is based on the internal implementation of local slant stack (LSS) operators optimally designed for each primary of the ray pairs. The LSS is applied in the direction of the horizontal slowness components of the arriving rays at the acquisition surface, where the size of the LSS is computed independently for each ray pair from its first Fresnel zone. Thus, primary reflection events sharing the same travel-time and the same surface directivity as the traced ray pairs are highly weighted while all other events (considered as noise) are simultaneously attenuated. The ability of this imaging technique to suppress noisy characteristics within the data, and in particular to attenuate different types of multiples contributes successfully in sub-basalt imaging in Padra area. Moreover the ability to decompose the 'specular' and 'diffraction' energy from the total scattered field obtained within the full azimuth directional gather using specular amplitude enhancement is the core component of using point- diffractor ray tracing which ensures maximum illumination of image points from both (a) all subsurface directions and (b) all surface source-receiver locations, accommodating all arrivals. Managing multi-pathing in wave-propagation successfully produces sub-basalt images in Padra area than Kirchhoff's migration which assumes single arrival.

Work Flow : The main steps of this workflow are:

1. Building an effective velocity model using (a) sonic logs from fifty (50) wells down to trap top, (b) update the model to include basalt velocity 'flooding' below the trap top and (c) finally using tomography within the trap to image the section below the trap top.
2. Full-azimuth sub-surface angle domain directional gather decomposition of full-azimuth 3D land seismic survey data.
3. Specular amplitude enhancement in the sub-surface Local Angle Domain (LAD) to image the intra-trap section.
4. Enhanced diffraction imaging by applying an appropriate diffraction filter to directional gathers.

The above workflow produces an enhanced specular reflection amplitude volume with good imaging of the intra trap section, and a high resolution diffraction volume for detection of small faults and fractures.

Data conditioning

Seismic data over in area of 50 sq. km was acquired with a bin size of 10 m X 10 m using orthogonal symmetric split spread shooting geometry in the year 2009-10. Common midpoint (CMP) gathers, which were used as input for vintage PSTM had almost 360 source-receiver azimuthal distribution as shown in Figure 3. This makes it an ideal input data set for full azimuth angle domain processing to be used in the present study. As a first step in data conditioning, residual static correction was done in shot domain to optimize the alignment of shallow reflections. Next, noise attenuation was done successively in shot, receiver and CMP domain.

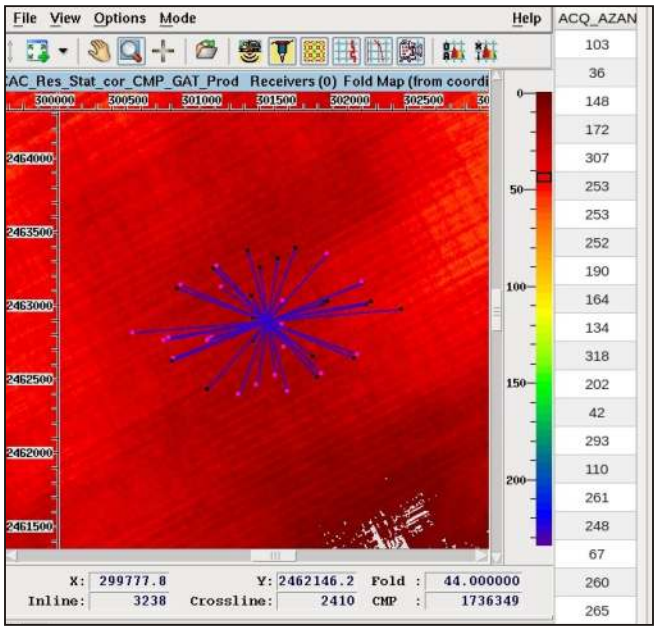

Figure 3: Azimuthal distribution of input CMP gather.

Velocity model building

Since the study area is a producing field, many sonic logs are available in the area, which penetrate few hundred meters below the trap top formation. Every sonic log shows a large increase in interval velocity in going from the overlaying sediments of the Olpad formation into the basement, which is quite normal in basaltic environment. So, using fifty suitably filtered sonic logs from the area, whose locations are shown in Figure 4, an initial geostatistical velocity model was built from floating datum to 500 m below the trap top.

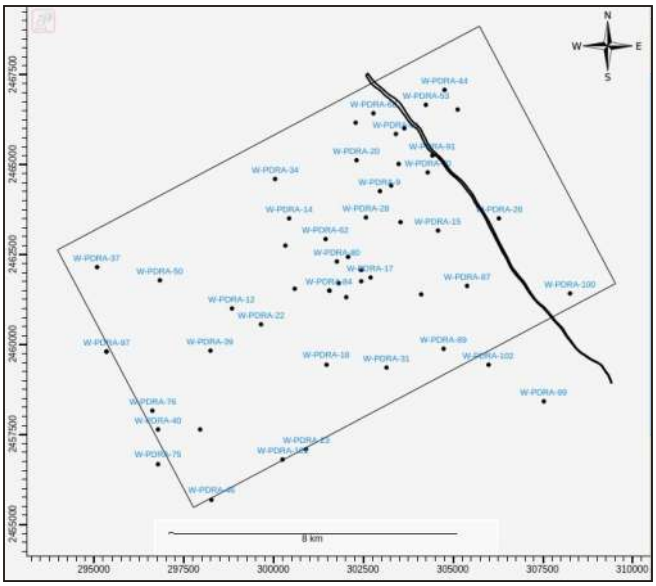

Figure 4: Location of the major fault and the sonic logs used to build initial geo-statistical model.

Secondly, velocity flooding was done within the basement formation using the high interval velocities obtained from sonic logs, with the aim of imaging intra-trap reflections. Next, the velocity models of the two zones (shallow sedimentary and deeper basement) were merged to form the starting depth velocity model which will be updated further using tomography.

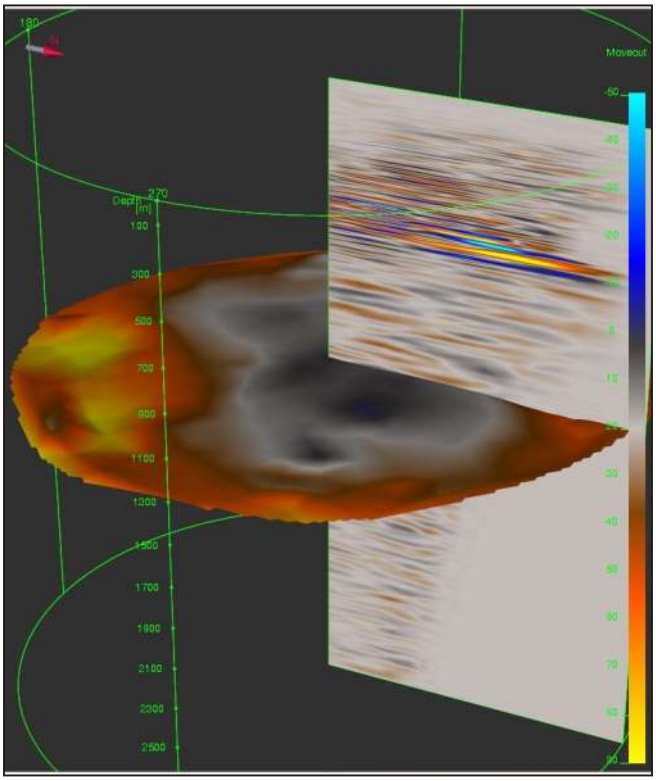

Figure 5: Residual moveout surface on 3D angle-azimuth reflection gather after five iterations

Since 3D reflection angle-azimuth gather is used for residual moveout calculation, residual moveout surfaces as shown in Figure 5. is used to update velocities. After five iteration, including last one as well-tie tomography the final depth velocity model is obtained as shown in Figure 6.

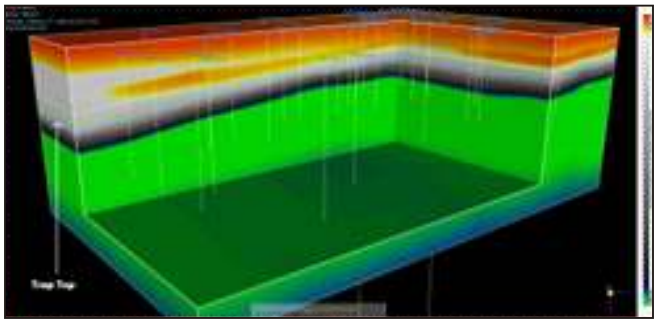

Figure 6: Final velocity model

Ray tracing using final depth interval velocity model at a depth far below the trap top formation depicts sufficient number of successful ray, having different emerging angle and azimuth as shown in Figure 7, validating both depth-velocity model and the migration aperture used. The intra-trap sub-surface point is illuminated by almost all 360 azimuthal directions, justifying the full-azimuth imaging.

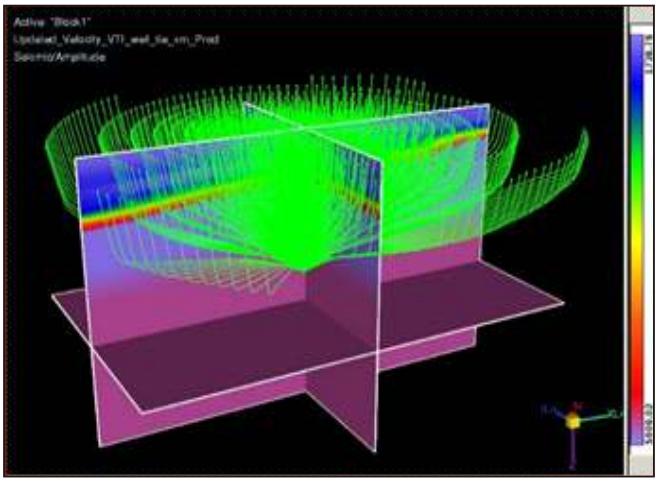

Figure 7: Ray tracing shows large number of rays emerging from an image-point well below the trap top are successfully reaching at the surface.

Full -azimuth LAD imaging

Due to application of Local Slant Stack (LSS), noise suppression and multiple attenuation are naturally performed within the imaging stage (Koren and Ravve, 2011). The vertical semblance plot along the Reflection angle-azimuth gather (Figure 8) shows clear, high-resolution, zero RMO coherency along the entire depth range.

In contrast the semblance of Kirchhoff PSDM offset gather is very noisy due to existence of multiples and noises (Figure 9) (Inozemstev, Koren, Galkin, 2015).

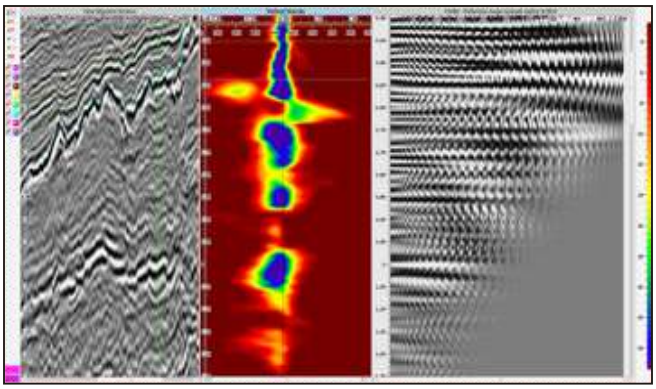

Figure 8: Stack-vertical semblance-reflection angle-azimuth gather. The high-resolution vertical semblance indicates the high level of continuity in the angle domain reflection events

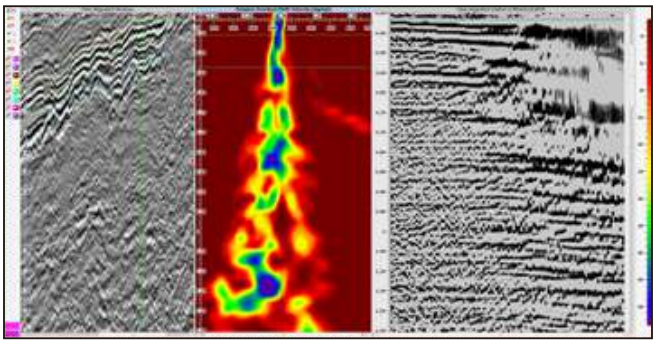

Figure 9: Stack-vertical semblance-Kirchhoff PSDM gather. Common offset gather shows chaotic semblance profile.

The ability of noise suppression and multiple attenuation directly within the imaging stage helps tremendously in sub-basalt imaging. The output of LAD processing is 5D LAD gather which can be subdivided into two sets of gathers, viz,

- 3D reflection gather (Figure 10)
- 3D direction gather (Figure 11)
  at the same CMP location of stack volume (Figure 12)

The trap top is clearly visible in both sets of gathers (~0.6 s). In reflection gather, azimuthal anisotropy is visible below the trap top. So it can be used further for velocity variation with azimuth (VVAZ) analysis. In direction gather, just below the trap top, fracture is distinctly observed in higher angles at a unique azimuth. In addition, new intra-trap reflections (1.4 s to 1.6 s) are observed in both reflection and directional gathers.

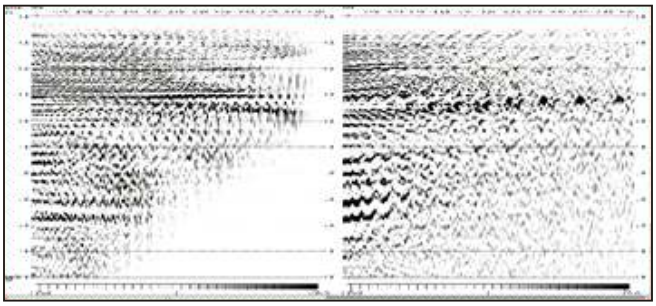

Figure 10: Reflection gather **Figure 11:** Directional gather

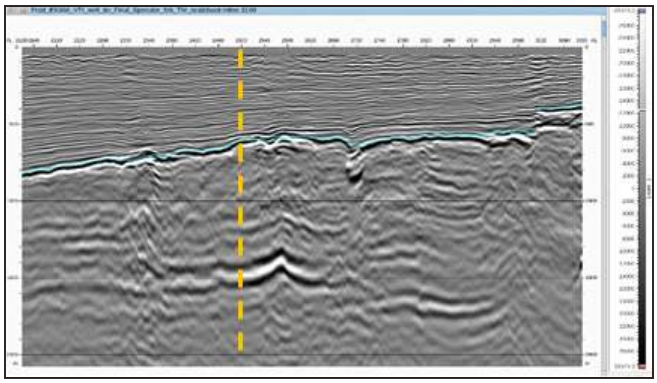

Figure 12: Stack section with the trap top horizon (yellow line shows gather location)

The stack section shows prominent reflections well below the trap top, proving the success of the adopted workflow in sub-basalt imaging.

Specular amplitude enhancement

Full-azimuth direction gathers contain directivity dependent information at each of the subsurface points. Thus, by applying a different specular/ diffraction weighted filter, one can separately produce specular image (Figure 13) and diffraction image (Figure 14) (Koren and Ravve, 2011).

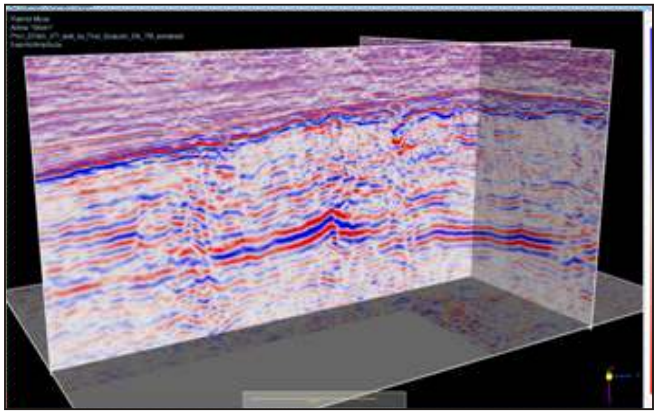

Figure 13: Specular stack volume in depth domain.

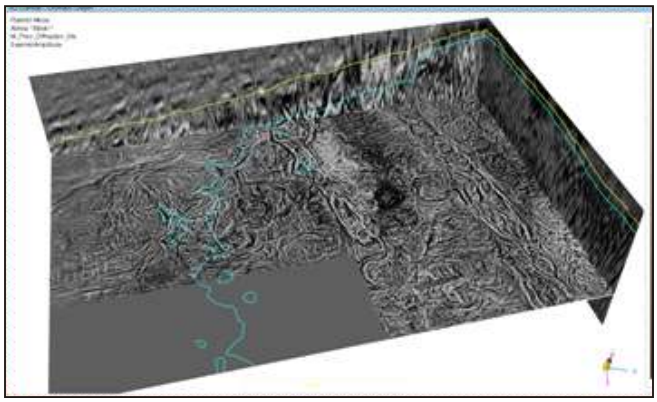

Figure 14: Diffraction stack volume in depth domain.

Specular image enhanced subsurface feature and made it more detailed and sharpened. This high resolution image

clearly imaged the deeper reflector well below the trap top. Diffraction image, on the other hand, shows enhanced imaging of spatially consistent geological discontinuities and higher resolution fault definition. Major NNW-SSE tending faults are distinctly visible in the diffraction volume. Distinct differences in fault pattern across the intersection of the depth slice with the trap top (shown by green line in Figure 14.) are clearly visible.

Image comparison in time domain

To compare full azimuth image with vintage one, specular stack is scaled to time and compared with vintage PSTM image (Figure 15).

Intra-trap reflector is clearly visible in the specular scaled stack which is so far not seen in any KPSTM vintages, justifying the supremacy of the adopted work-flow in sub-basalt imaging.

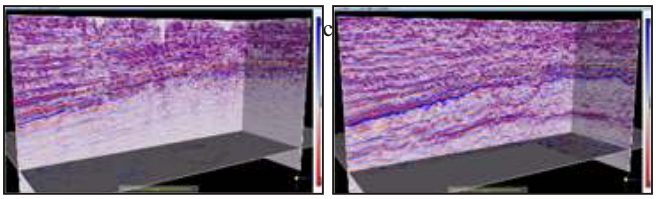

Figure 15: Vintage KPSDM (left) and specular stack (right) in time domain

Conclusions

Sub-basalt imaging using full azimuth sub-surface angle domain processing generates:

- A high resolution diffraction dataset that more accurately captures spatial discontinuities related to fault and fractures.
- An enhanced and sharpened specular dataset that imaged a previously unrecognized prominent intra-Deccan reflector.

Acknowledgement

Authors wish to thank ED-Basin Manager WOB, ONGC; for permission to publish this paper.

References

Biswas, S. K., 1982, Rift basins in western margin of India and their hydrocarbon prospects with special reference to Kutch Basin, AAPG Bulletin, 66, no.10,1497-1513.

Koren, Z., and Ravve, I., 2011, Full-azimuth subsurface angle domain wavefield decomposition and imaging Part I : Directional and reflection image gathers, Geophysics, 76, no.1, S1-S13, https://doi.org/10.1190/1.3511352.

Inozemtsev, A., Koren, Z., and Galkin, A., 2015, Noise suppression and multiple attenuation using full-azimuth angle domain imaging: case studies, First Break, 33, 81-86.